The Journal of Immunology

# Peptidic Termini Play a Significant Role in TCR Recognition

Bo Wang, Ashawni Sharma, Robert Maile, Mohamed Saad, Edward J. Collins and Jeffrey A. Frelinger



*J Immunol* 2002; 169:3137-3145; ;
doi: 10.4049/jimmunol.169.6.3137
http://www.jimmunol.org/content/169/6/3137



*The Journal of Immunology* is published twice each month by
The American Association of Immunologists, Inc.,
1451 Rockville Pike, Suite 650, Rockville, MD 20852

Print ISSN: 0022-1767 Online ISSN: 1550-6606.

# Peptidic Termini Play a Significant Role in TCR Recognition[1]

**Bo Wang,[2]* Ashawni Sharma,[2]* Robert Maile,* Mohamed Saad,* Edward J. Collins,*† and Jeffrey A. Frelinger[3]***

**TCR recognition of class I MHC is dependent on the composition of the antigenic peptide and the MHC. Single amino acid substitutions in either the MHC or the peptide may dramatically alter recognition. While the major interactions between TCR and the peptide/MHC complex appear to be focused on the complementarity-determining region (CDR)3, it is also clear from the cocrystal structure of class I MHC and TCR that the amino and carboxyl ends of the peptide may play a role through interactions with the CDR1. In this work we show that gp33 variants substituted at the peptidic termini at the putative CDR1 contact regions show improved recognition in B6 mice. The rank order of recognition is different using the P14 transgenic T cells, suggesting that one reason for improved recognition is a change in the TCR repertoire that recognizes the peptide. However, the affinity of the TCR by some of the peptide/MHC complex with increased recognition is improved, as shown by increased tetramer binding to P14 T cells. These substitutions at the termini of the peptide-binding cleft cause localized conformational changes as seen by changes in mAb binding and crystallographic structures. The different peptide structures also show different conformations in the center of the peptide, but these are shown to be energetically similar and thus most likely have no significance with respect to TCR recognition. Therefore, small conformational changes, localized to the CDR1 contact regions, may play a significant role in TCR recognition.** ***The Journal of Immunology*****, 2002, 169: 3137–3145.**

Cytotoxic $CD8^+$ T cells recognize foreign peptides bound by MHC class I molecules (1, 2). The interaction involves three components: TCR on the surface of T cells, MHC class I on the surface of APC, and peptide Ags bound to MHC class I molecules. The recognition of peptide/MHC (pMHC)[4] complexes by TCR on cytotoxic CD8 T cells leads to activation of $CD8^+$ T cells and the lysis of the cells presenting the antigenic peptide.

Structural studies of pMHC have provided detailed information about the conformation of peptide when bound to MHC class I molecules (3–8). The peptide-binding groove of MHC class I molecules is composed of two helices on top of an eight-strand antiparallel $\beta$-pleated sheet (9). The peptide-binding groove has been described as containing various binding pockets (pockets A–F) that have specific roles in binding the antigenic peptides (10). Peptides bind to MHC class I molecules with the amino acids at the amino and carboxylate termini buried in pockets A and F, respectively, independent of the peptide sequence. The shape and charge of the remaining pockets are dependent on the highly polymorphic amino acids from one MHC allele to another (8, 11). The composition of the pockets selectively determines the spectrum of peptides in terms of length and amino acid composition that may bind to a given allotype (2, 12, 13).

TCR recognition is dependent on the primary sequence of both the antigenic peptide and the MHC (14–16). Single amino acid substitutions in either the MHC or the peptide may dramatically alter recognition by T cells (9). Recently, the cocrystal structures of several $\alpha\beta$ TCR/class I MHC complexes from both human and mouse have been determined (17–22). These studies demonstrated that all TCRs studied interact with the pMHC complex in a diagonal orientation with the complementarity-determining region (CDR)1 of the $\alpha$-chain near the N terminus of the peptide and the CDR1 of the $\beta$-chain over the C terminus of the peptide. The CDR2 of the TCR $\alpha$- and $\beta$-chains interact with the two $\alpha$ helixes and the CDR3 of both $\alpha$- and $\beta$-chains are positioned over the center of pMHC complex. This orientation explains the observed diversity in the CDR3. Apparently, the peptide specificity of T cells is primarily determined by the interaction between the CDR3 of TCR and the peptide side chains, which protrude out of the peptide binding groove of MHC class I molecules toward TCR CDR3 (20, 22, 23). Although the CDR1 appear poised over the P1 and P9 positions, only one (HLA-B7) of the four TCR class I MHC cocrystals shows specific contacts with the P1 residue. None of the four interacts with the P9 residue (17, 19–21).

While the major interactions between TCR and pMHC appear to be focused on the CDR3, it is also clear that the amino and carboxyl ends of the peptide may play a role through interactions with the CDR1 and that these interactions may have a significant impact on T cell recognition of peptide. Results from our laboratory and others using HLA-A2 suggested that changes in the P1 and P9 positions of the peptide could result in increased affinity of the peptide for the MHC and enhanced recognition by T cells. Accordingly, we decided to test this idea further in a well-described murine system. We made substitutions of a $D^b$-restricted antigenic epitope (LCMV gp33) at the N and C termini and studied the impact of the substitutions on the crystallographic structure of the pMHC complex, binding of specific Abs, and recognition by $CD8^+$ T cells. Unexpectedly, our results demonstrate that the N and C termini dynamically contribute to the conformation of

Departments of *Microbiology and Immunology and †Biochemistry and Biophysics, University of North Carolina, Chapel Hill, NC 27599

Received for publication April 12, 2002. Accepted for publication July 12, 2002.

The costs of publication of this article were defrayed in part by the payment of page charges. This article must therefore be hereby marked *advertisement* in accordance with 18 U.S.C. Section 1734 solely to indicate this fact.

[1] This work was supported by National Institutes of Health Grants AI 20288 and GM 67143.

[2] B.W. and A.S. contributed equally to this manuscript.

[3] Address correspondence and reprint requests to Dr. Jeffrey A. Frelinger, Department of Microbiology and Immunology, University of North Carolina, CB #7290, 804 Mary Ellen Jones Building, Chapel Hill, NC 27599. E-mail address: jfrelin@med.unc.edu

[4] Abbreviations used in this paper: pMHC, peptide/MHC; CDR, complementarity-determining region; RAG, recombination-activating gene; $\beta_2$-m, $\beta_2$-microglobulin.



0022-1767/02/$02.00

pMHC complex, as well as the affinity of TCR with the pMHC complex, resulting in a modulation of the immune response.

## Materials and Methods

### *Animals*

C57BL/6 mice were purchased from Charles River Breeding Laboratories (Raleigh, NC). P14 TCR-transgenic mice (B6;D2-TgN (TCR-LCMV) 327 Sdz) expressing a transgenic TCR specific for LCMV gp33 peptide (33–41) (24) were purchased from The Jackson Laboratory (Bar Harbor, ME) and further backcrossed to C57BL/6 mice six times. P14 TCR-transgenic mice were crossed with mice deficient in $\beta_2$-microglobulin ($\beta_2$-m) expression (B6.129P2-*B2m*$^{tm1Unc}$; $\beta_2$-m knockout) and recombination-deficient mice (B6.129S7-*Rag1*$^{tmMom}$; recombination-activating gene (RAG) knockout), respectively, to produce P14 TCR-transgenic mice lacking the $\beta_2$-m expression (P14/$\beta_2$-m$^{0/0}$) and P14 TCR-transgenic mice deficient in the RAG expression (P14/RAG$^{0/0}$).

### *Peptides*

All peptides were synthesized using F-moc chemistry by the Peptide Synthesis Facility (Microbiology and Immunology, University of North Carolina, Chapel Hill, NC). Peptides were purified to >95% by reversed-phase chromatography. Characterization of the peptide was completed using matrix-assisted laser desorption time of flight mass spectrometry. Peptides used are shown in Table I.

### *Preparation of gp33 variant/D$^b$ complexes*

gp33 variant/D$^b$ complexes were prepared as described previously (25). Briefly, residues 2–274 of D$^b$ and murine $\beta_2$-m were produced in *Escherichia coli* as inclusion bodies and folded in vitro. Peptide, solubilized $\beta_2$-m, and D$^b$ H chain were rapidly diluted into folding buffer (100 mM Tris (pH 8), 400 mM L-Arg, 10 mM reduced glutathione, 1 mM oxidized glutathione, and protease inhibitors) at molar ratios of 10:2:1. The folding buffers were incubated at 10°C for 36–48 h and then concentrated using an ultrafiltration cell (Amicon, Beverly, MA). The peptide/D$^b$ complexes were purified by HPLC gel filtration chromatography (Biosep-Sec-S2000; Phenomenex, Torrance, CA).

### *Tetramers*

The tetramers used in this study were prepared using the procedure previously described (26). Plasmid-encoding D$^b$ with a BirA recognition sequence at the C terminus was a gift provided by Dr. J. D. Altman (Emory College of Medicine, Atlanta, GA). Inclusion bodies were prepared and protein was folded in vitro as described above. Purified peptide/D$^b$ complexes were biotinylated according to the manufacturer's instructions (Avidity, Denver, CO). Excess biotin was removed by size exclusion chromatography with Sephadex G-25 (Bio-Rad, Hercules, CA). The extent of the biotinylation was assessed by a gel shift assay. Protein was incubated with streptavidin (Sigma-Aldrich, St. Louis, MO), added to sample buffer without boiling, and examined for a mobility shift by Coomassie-stained SDS-PAGE. All pMHC complexes were bound to PE-labeled ultra-avidin (Leinco, St. Louis, MO) for use in flow cytometric studies and unconjugated ultra-avidin for proliferation studies.

### *Cytotoxicity assay*

Cytotoxic assays in this study were performed in a standard 4-h $^{51}$Cr release assay described previously (26). In brief, either B6 or P14 TCR-transgenic mice were infected with LCMV (Armstrong strain). Seven days after virus infection, splenocytes were isolated and used as effector cells. EL4 cells were labeled with $^{51}$Cr, pulsed with various concentrations of peptides, and used as target cells. Peptide-pulsed targets are used instead of continuous exposure to peptide to eliminate the possibility of fratricide by the CTL effectors. Effectors and targets at an E:T ratio of 50 were incubated at 37°C in 5% $CO_2$ for 4 h and the supernatant was harvested. $^{51}$Cr released was counted in a Cobra Auto Gamma Counter (Packard, Downers Grove, IL). Specific lysis was calculated as previously described. Each data point represents the average of triplicate measurements.

Table I. *Peptides used in this study*

| Peptide | Sequence |
|---|---|
| gp33 | KAVYNFATC |
| C9M | KAVYNFATM |
| K1S | SAVYNFATC |
| K1A/C9M | AAVYNFATM |
| K1S/C9M | SAVYNFATM |

### *Proliferation assay*

Spleen cells prepared from P14/RAG$^{0/0}$ or P14/$\beta_2$-m$^{0/0}$ mice were cultured in 96-well flat-bottom plates at $4 \times 10^5$ cells per well in the presence of increasing concentrations of tetramers, as indicated in the figures. The cultures were incubated at 37°C in 5% $CO_2$ for 2–3 days and pulsed with 1 $\mu$Ci (6.7 Ci/mM) of [$^3$H]thymidine per well for the last 10 h. Cells were harvested onto glass filter by using a multiple sample harvester (Otto Hiller, Madison, WI). Incorporation of [$^3$H]thymidine was measured by a scintillation counter (Beckman Coulter, Palo Alto, CA).

### *Peptide binding assay*

Peptide binding assays were performed as described (27). Briefly, TAP-deficient T2/D$^b$ cells (0.174 × CEM T2 (28), transfected with a cDNA for H-2D$^b$) were incubated with the indicated concentrations of peptides at 37°C in 5% $CO_2$ overnight. Cells were washed and incubated with either 28.14.8s (29) or 28.8.6s (30) supernatants on ice. The binding of mAbs was examined by staining with PE-labeled anti-mouse IgG Ab (BD PharMingen, San Diego, CA) and analyzed by flow cytometry using Cyclops software (Cytomation, Ft. Collins, CO). Fluorescence due to isotype-matched control staining was subtracted from the fluorescence for each concentration of peptide as background.

### *Crystallization, data collection, and data processing*

All complexes were crystallized using the hanging drop vapor diffusion method. The hanging drop for all three complexes contained a 1/1 mixture of the reservoir solution and 10 mg/ml protein in 25 mM MES buffer (pH 6.5). The reservoir solution contained 10–20% PEG8000 in 25 mM MES buffer (pH 6.5) and 1% dioxane. For all complexes, microseeds of Flu/D$^b$ (ASNENMTEM) peptide were used to obtain diffracting quality crystals. Crystallographic data for all three complexes were collected on a rotating anode Rigaku RU200 (Rigaku Instruments, Tokyo, Japan) and Image plate RAXIS IIC (Molecular Structure, The Woodlands, TX) using Cu K$\alpha$ radiation. The data for all the complexes were processed using the programs DENZO and SCALEPACK (31). Data statistics are shown in Table II.

### *Structure determination and refinement*

All three structures were determined by molecular replacement using AMoRe within the CCP4 program suite (32). The complex of p1027/D$^b$ (Brookhaven Protein Data Bank accession no. 1bz9) was used as the search model (25). The search model was divided into two pieces, peptide binding superdomain ($\alpha_1\alpha_2$) and $\alpha_3$ domain, $\beta_2$-m L chain. Computational refinement was performed using CNS. Rigid body refinement was performed using three domains ($\alpha_1\alpha_2$ peptide-binding superdomain, $\alpha_3$, and $\beta_2$-m) as separate rigid bodies. Seven rounds of torsional dynamics for C9M and K1S/C9M and six rounds for K1A/C9M were performed using CNS. The peptide was not included in the initial rounds of refinement as an internal control for model bias. Two-fold noncrystallographic averaging, histogram matching, and solvent flattening were applied using DM (32) to generate electron density maps. Manual model building was performed using the model building software O (33) with electron density maps of 2Fo-Fc and Fo-Fc coefficients. The refinement statistics are given in Table II.

## Results and Discussion

T cell responses to LCMV have been well characterized. B6 mice infected with LCMV generate a strong cytotoxic response with a dramatic expansion and intense activation of CD8$^+$ T cells (up to 50% of CD8$^+$ T cells) (34). The vast majority of these activated CD8$^+$ cells are specific for three viral epitopes (34, 35). One of the dominant epitopes is LCMV gp33, derived from the glycoprotein (36) and restricted by D$^b$. To determine the impact of the amino acids at the N and C termini of Ag peptide on the immune response, we made a series of 35 peptides substituted at either position 1 or position 9 of the LCMV gp33 epitope. We were particularly interested in the five variant peptides of LCMV gp33 shown in Table I. These peptides were chosen because they were stable on the surface when bound to D$^b$ and could be recognized by gp33-specific CTL. Variants were made by substituting serine for lysine at position 1 (K1S), alanine for lysine at position 1 (K1A),

Table II. *Summary of crytallographic analysis of peptide/D$^b$ complexes*

| | C9M | K1A/C9M | K1S/C9M |
|---|---|---|---|
| Data statistics | | | |
| Cell dimensions | a = 47.26 Å<br>b = 68.91 Å<br>c = 81.75 Å<br>$\alpha$ = 72.92°<br>$\beta$ = 73.24°<br>$\gamma$ = 69.97° | a = 47.22 Å<br>b = 68.64 Å<br>c = 81.53 Å<br>$\alpha$ = 74.57°<br>$\beta$ = 73.08°<br>$\gamma$ = 69.86° | a = 47.01 Å<br>b = 66.90 Å<br>c = 80.41 Å<br>$\alpha$ = 75.10°<br>$\beta$ = 72.90°<br>$\gamma$ = 69.28° |
| Molecules/asymmetric units | 2 | 2 | 2 |
| Resolution (Å) | 2.7 | 2.65 | 2.6 |
| $R_{merge}$ (%)[a] | 11.9 (35.4) | 12.5 (20.6) | 9.4 (35.7) |
| $<I/\sigma>$ | 5.20 (1.98) | 6.51 (3.93) | 9.01 (2.48) |
| Unique reflections | 22,352 | 24,299 | 25,600 |
| Total observations | 99,827 | 104,494 | 109,795 |
| Completeness (%) | 89.8 (85.6) | 93.8 (85.4) | 96.9 (95.2) |
| Refinement statistics | | | |
| Resolution (Å) | 50–2.7 | 50–2.65 | 50–2.6 |
| $R_{work}$ (%)[b] | 24 (21,198) | 24.6 (23,056) | 25 (24,296) |
| $R_{free}$ (%) | 28.6 (1,154) | 29.2 (1,243) | 30.3 (1,304) |
| Error (Å)[c] | 0.37 | 0.38 | 0.37 |
| Non-hydrogen atoms | 6,294 | 6,286 | 6,288 |
| <RS fit> (%)[d] | 75.7 | 73.2 | 78.2 |
| Average B factor (Å)[e] | 26.9 | 31.6 | 27.5 |
| No. of waters | 32 | 12 | 14 |
| RMSD bonds (Å) | 0.008 | 0.008 | 0.008 |
| RMSD angles (degrees) | 1.4 | 1.4 | 1.4 |
| Ramachandran (%) | | | |
| Most favorable | 84 | 87.5 | 82.5 |
| Additionally allowed | 14.4 | 10.6 | 15.4 |
| Generously allowed | 1.7 | 2 | 2.1 |
| Disallowed | 0 | 0 | 0 |

[a] $R_{merge} = \Sigma_{hkl} \Sigma_i |I_i - \langle I \rangle| / \Sigma_{hkl} \Sigma_i I_i$, where $I_i$ is the observed intensity and $\langle I \rangle$ is the average intensity of multiple observations of symmetry-related reflections.

[b] $R = \Sigma_{hkl} |F_{obs}| - k |F_{cal}| / \Sigma_{hkl} |F_{obs}|$, where $R_{free}$ is calculated for a randomly chosen 5% of reflections and $R_{work}$ is calculated for the remaining 95% of reflections used for structure refinement. Numbers in parentheses refer to the number of structure factors used in the measurements.

[c] Error is the mean coordinate error estimate based on maximum likelihood measurements (59).

[d] RS fit is the average real space fit of all atoms on an electron density map from DM with 2-fold noncrystallographic averaging, histogram matching, and solvent flattening.

[e] Number in parentheses refers to the highest resolution shell. It is 2.87–2.70 Å for C9M, 2.82–2.65 Å for K1A/C9M, and 2.76–2.6 Å for K1S/C9M.

or methionine for cysteine at position 9 (C9M), or combining both of these substitutions to produce a doubly substituted peptides (K1S/C9M or K1A/C9M).

To examine how the substitutions affect effector function of a polyclonal set of activated CD8$^+$ T cells, splenocytes from B6 mice infected with LCMV were used as cytotoxic effector cells. Cytotoxic activity was assessed in a standard 4-h $^{51}$Cr release assay against EL4 target cells pulsed with wild-type peptide (LCMV gp33) or the variants. Representative results are presented in Fig. 1. Three groups are apparent. Target EL4 cells pulsed with K1S/C9M were recognized much more efficiently than any other peptides. K1A/C9M and K1S peptides, although not as effective as K1S/C9M, sensitized targets more efficiently than those pulsed with wild-type gp33 or C9M. Substitutions with other amino acids at positions 1 and 9 either abrogated or did not affect the cytotoxic response of activated CD8 T cells from LCMV-infected mice (data not shown).

Several possibilities could account for the increased lysis of target cells sensitized with variant peptides. First, the substitutions in the LCMV gp33 peptide could change the affinity of the peptides for D$^b$. This greater affinity would increase the effective concentration of the pMHC on the surface of the APC. Second, the variant pMHC complex may have a higher affinity with the specific TCR (a clone or limited number of clones). Third, a conformational change in the pMHC complex may be required to accommodate the substitution in the peptide and this new conformation may be recognized by a broader TCR repertoire.

To distinguish among the above possibilities, we first measured the binding of the peptides to D$^b$. As can be seen in Fig. 2, there is not a significant difference in loading of peptides on to D$^b$ molecules, although C9M does bind slightly better. In addition, we measured the surface stability of gp33, C9M, and K1S. All these peptides have half-lives bound to D$^b$ >24 h (data not shown), indicating that differences in half-lives of the peptides are not likely to be the cause of the differential recognition. All of these peptides bind well to D$^b$ as compared with poor immunogens such as the HY Ag (R. Maile, unpublished data). Thus, we conclude that the differences in binding to D$^b$ is not the primary reason for differences in recognition by B6 splenocytes.

We next studied the effect of the substitutions on a single TCR using LCMV gp33-specific CD8$^+$ T cells to evaluate potential changes in pMHC/TCR affinity on cytotoxicity and proliferation. Spleen cells from P14/RAG$^{0/0}$ mice were used as effector cells after infection with LCMV 7 days previously. Specific lysis was measured using EL4 cells sensitized with LCMV gp33 or its variants in a standard 4-h $^{51}$Cr release assay. In contrast to the response of B6 mice (Fig. 1), P14 transgenic T cells recognize C9M at a concentration ~10-fold lower than for gp33 (Fig. 3*A*). P14 T cells showed weaker activity to K1S in that they require almost 1000-fold more peptide to generate the same lysis as generated by gp33.

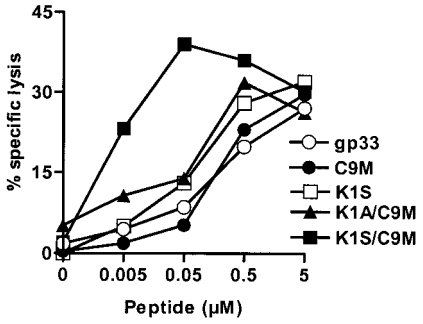


**FIGURE 1.** P1 and P9 variants of gp33 are more efficiently lysed by B6 splenocytes. B6 mice were infected with LCMV 7 days before the assay. Spleen cells were prepared and used as effector cells. EL4 cells were pulsed with gp33 (○), C9M (●), K1S (□), K1S/C9M (■), or K1A/C9M (▲) at the indicated concentrations. CTL response against peptide-pulsed EL4 cells was measured in a standard 4-h $^{51}$Cr release assay at an E:T ratio of 50:1.

Double substitution caused unexpected deleterious consequences. Peptides KIS/C9M and K1A/C9M are not recognized as well as C9M. K1A/C9M is recognized ~10-fold worse than gp33 and 100-fold worse than C9M, while K1S/C9M is equivalent to gp33 but 10-fold less than C9M. The deleterious effects of the P1 substitution clearly caused secondary effects, which are not correctable by substitutions at the P9 end of the peptide. However, it must be noted all of these peptides can sensitize EL4 cells to killing by B6 splenocytes (Fig. 1). Although the pMHC/TCR cocrystal structures rarely show contacts directly with the P1 residue, previous work from our laboratory and others has shown that substitution of P1 residue affects the recognition by TCR (37–39). T cells from LCMV-infected B6 mice and P14/RAG$^{0/0}$ mice respond quite differently toward these variant peptides. These data suggest that the substitutions at either position 1 or position 9 of LCMV gp33 cause a conformational change in the pMHC complex that allows recognition by a broader T cell repertoire from LCMV-infected B6 mice. However, there appear to be differences in recognition by P14 TCR that may be accounted for by changes in affinity between pMHC and TCR. Because the substitutions did not abrogate the recognition by P14 TCR, they may change the affinity of TCR for pMHC complex, e.g., by increasing affinity for C9M and decreasing affinity for K1S.

Our previous work has demonstrated that pMHC tetramers can efficiently activate naive CD8$^+$ T cells in vitro (26). Recently, Lim et al. (40) reported an inconsistency between cytotoxic effector

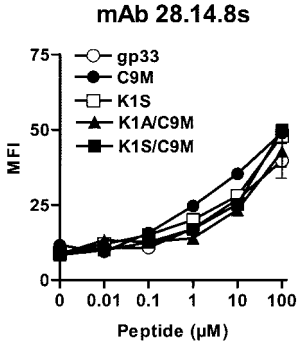


**FIGURE 2.** Improved recognition of gp33 variants is not due to improved binding to D$^b$. T2/D$^b$ cells were incubated with peptides at the indicated concentrations overnight and stained with mAb 28.14.8s hybridoma supernatants. The binding of the primary Ab is shown by staining with a secondary PE-conjugated anti-mouse IgG Ab (BD PharMingen). Data show the mean fluorescence detected by flow cytometry.

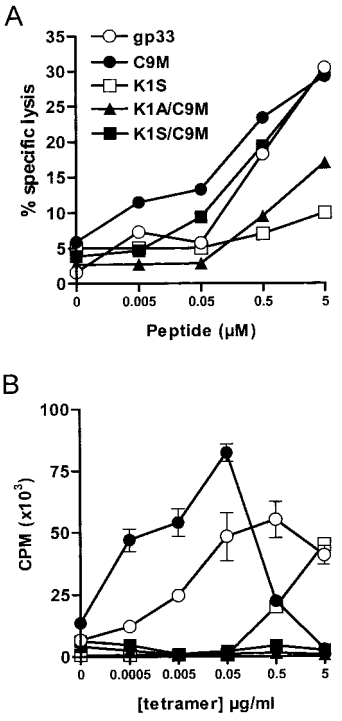


**FIGURE 3.** P1 and P9 gp33 substitutions affect the activity of P14 T cells differently from B6 splenocytes. *A*, P14/RAG$^{0/0}$ transgenic mice were infected with LCMV 7 days before the assay. Spleen cells were prepared and used as effector cells as described in *Materials and Methods*. Target EL4 cells were pulsed with gp33 (○), C9M (●), K1S (□), K1S/C9M (■), or K1A/C9M (▲) at the indicated concentrations. CTL response was measured in a standard 4-h $^{51}$Cr release assay at an E:T ratio of 50:1. B. Spleen cells from P14/RAG$^{0/0}$ mice were stimulated for 48 h with concentrations of tetramer indicated and labeled with 1 $\mu$Ci of [$^3$H]thymidine per well overnight. Proliferation was measured by the incorporation of [$^3$H]thymidine. Individual data points represent the average cpm of triplicate.

function and proliferation of T cells. To examine whether these substitutions may have altered effects on proliferation as compared with lysis, we assayed proliferation of P14 transgenic T cells stimulated with tetramers carrying either wild-type LCMV gp33 or its analogs. Naive spleen cells were isolated from P14/RAG$^{0/0}$ mice and stimulated with various tetramers as indicated in Fig. 3*B*. Proliferation of T cells was measured by incorporation of [$^3$H]thymidine. The tetramer C9M/D$^b$ stimulates proliferation of T cells from P14/RAG$^{0/0}$ mice more efficiently than gp33/D$^b$ and 100-fold better than K1S/D$^b$. The same T cells did not proliferate nearly as well after stimulation by tetramers K1S/D$^b$ or K1A/C9M/D$^b$, even at high concentrations. One possible explanation for the discrepancy seen between cytotoxicity and proliferation is that different strength signals are required for these activities. Lim et al. (40) demonstrated that the engagement of costimulatory molecules is necessary for proliferation of the T cell clones used in their experiments. We see no such effect (26). The question that remained was whether the difference in ligands was the affinity of the pMHC for the TCR.

To determine whether the substitutions introduced at position 1, position 9, or both positions changed the affinity of the pMHC complex for P14 TCR, we stained P14/RAG$^{0/0}$ T cells with fluorescently labeled tetramers and nonblocking anti-CD8 Ab. The fluorescence intensity was measured by flow cytometry. As shown in Fig. 4, the staining profile of P14 TCR-transgenic T cells by various tetramers was significantly different. C9M/D$^b$ tetramer stained P14 TCR-transgenic T cells better than the gp33/D$^b$ tetramer. In

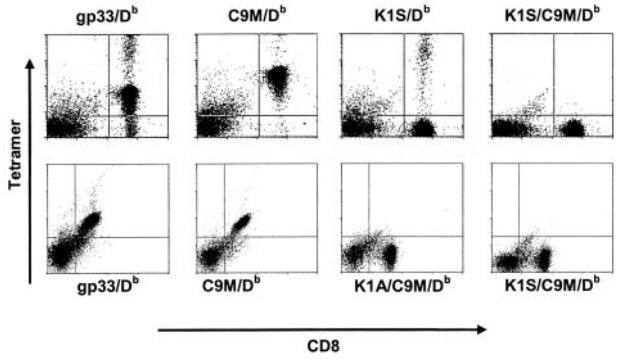


**FIGURE 4.** The substitutions at P1 and P9 change the affinity of P14 TCR with its ligands. Splenocytes from P14/RAG$^{0/0}$ mice were stained with PE-conjugated tetramers and FITC-labeled anti-CD8 mAb (53–6.7), then analyzed by flow cytometry. Shown are the profiles of P14 transgenic T cells stained with different tetramers as indicated on the *top* of the panels. Similar staining patterns were obtained with increased concentrations of tetramer. The experiments were performed on different days, so staining by CD8 and tetramer are not equivalent between experiments but are consistent within the experiments. The populations of cells stained very intensely with tetramer in the *upper panels* are likely staining by aggregated tetramers.

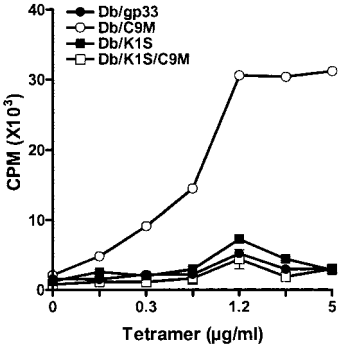


**FIGURE 5.** P14 T cells are activated by high-affinity tetramer without CD8 coreceptor involvement. Spleen cells were prepared from P14/$\beta_2$-m$^{0/0}$ mice and stimulated with various tetramers at different concentrations. Proliferation was measured as described in Fig. 3. Data show the average cpm of triplicate. Over 80% of the T cells in the cultures that express the V$\alpha$2 transgene are CD4$^-$CD8$^-$.

contrast, K1S/D$^b$, K1S/C9M/D$^b$, and K1A/C9M/D$^b$ tetramers hardly stained the P14 transgenic T cells at all. The profile presented in Fig. 4 did not change with higher concentrations of tetramers. These data demonstrate that the substitutions resulted in a change in affinity of TCR for pMHC complex and that the highest affinity to P14 TCR was conferred by the C9M substitution. Conversely, the substitutions at P1, K1A, and K1S reduced the apparent affinity for the P14 TCR. These data suggest that the change in P14 reactivity is due to a change in the affinity of the pMHC complex for the TCR.

One of the functions of CD8 coreceptor (in addition to its involvement in signal transduction) may be to enhance the interaction between TCR and the pMHC complex (41–44). In this study we wanted to know whether the increased affinity of C9M/D$^b$ with P14 TCR might overcome the coreceptor dependence. We introduced the P14 TCR transgene onto the $\beta_2$-m-deficient background to produce P14/$\beta_2$-m$^{0/0}$ mice. While positive selection is inefficient in these mice, ~50% of CD3-positive T cells express the transgenic TCR and lack any coreceptor; the other 50% express CD4 and the transgenic TCR (data not shown). P14/$\beta_2$-m$^{0/0}$ spleen cells were stimulated in vitro with various tetramers, as indicated in Fig. 5, and proliferation was measured. Interestingly, while gp33 tetramer induced proliferation of wild-type P14 T cells, it was unable to do so in the P14/$\beta_2$-m$^{0/0}$ T cells. However, splenocytes from P14/$\beta_2$-m$^{0/0}$ mice proliferated when stimulated with C9M/D$^b$ tetramer (Fig. 5, ○). Other tetramers, including gp33/D$^b$, failed to induce proliferation (Fig. 5). Because the T cells in the P14/$\beta_2$-m$^{0/0}$ mice are either double negative or CD4 positive, these data suggest that the affinity of C9M/D$^b$ for the P14 TCR is high enough to not require CD8 for function. Similarly, a differential requirement of CD4 coreceptor has been found in CD4 T cell activation (45). These results further show that substitution of LCMV gp33 at its C and N termini caused a change in affinity of P14 TCR for its ligands, mainly higher affinity for C9M/D$^b$ and lower affinity for K1S/D$^b$ and K1S/C9M/D$^b$, compared with gp33/D$^b$. The coordinates for C9M/D$^b$ (1FFN), K1S/C9M/D$^b$ (1FFP), and K1A/C9M/D$^b$ (1FFO) have been deposited with the protein data bank at the Research Collaboratory for Structural Bioinformatics.

The data from the above experiments raise an important question as to how the substitutions at the positions 1 and 9 impact the affinity between TCR and its ligands. The change in affinity between TCR and the pMHC complex could be simply due to the strength of the interaction between the residues of the CDR1 of TCR and the side chains of peptide substitutions. However, it is also possible that the substitutions induce a structural modification of the peptide backbone, which would propagate to the center of the peptide, which is the area that binds to the CDR3 loops.

Several studies have shown that subtle conformational changes can be detected by mAbs (46–48). We have examined the conformation of MHC class I D$^b$ bound with different mutant peptides using mAbs specific for D$^b$ molecules. The T2D$^b$ cell line is an H-2D$^b$ transfectant of the human T and B cell hybrid (T2), which is deficient in both TAP1 and TAP2 genes. Because surface stabilization of D$^b$ molecules is peptide dependent, T2D$^b$ cells were incubated with LCMV gp33 and analog peptides and surface levels of D$^b$ molecules were evaluated by flow cytometry after staining with D$^b$-specific mAbs. The mAb 28.14.8s recognizes an epitope located in the $\alpha_3$ domain of the D$^b$ molecule, independent of D$^b$ $\alpha_1$ and $\alpha_2$ conformation (29). This epitope allowed us to measure stabilization of D$^b$ relative to peptide concentration independently of the sequence of the peptide, as shown in Fig. 2. However, mAb 28.8.6s is specific for an epitope formed by $\alpha_1$ and $\alpha_2$ regions of D$^b$ molecules somewhere near the N terminus of the peptide (49). Thus, the recognition of D$^b$ molecules by mAb 28.8.6s could be

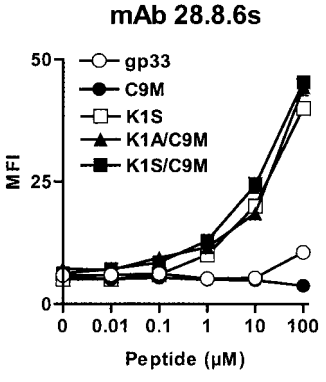


**FIGURE 6.** mAb detects a conformational change in pMHC complex with gp33 variants. T2/D$^b$ cells were incubated with peptides at different concentrations overnight and stained with supernatant from mAb 28.8.6s. The binding of the primary Ab is revealed by staining with a secondary PE-conjugated anti-mouse IgG Ab (BD PharMingen). Data show the mean fluorescence detected by flow cytometry.

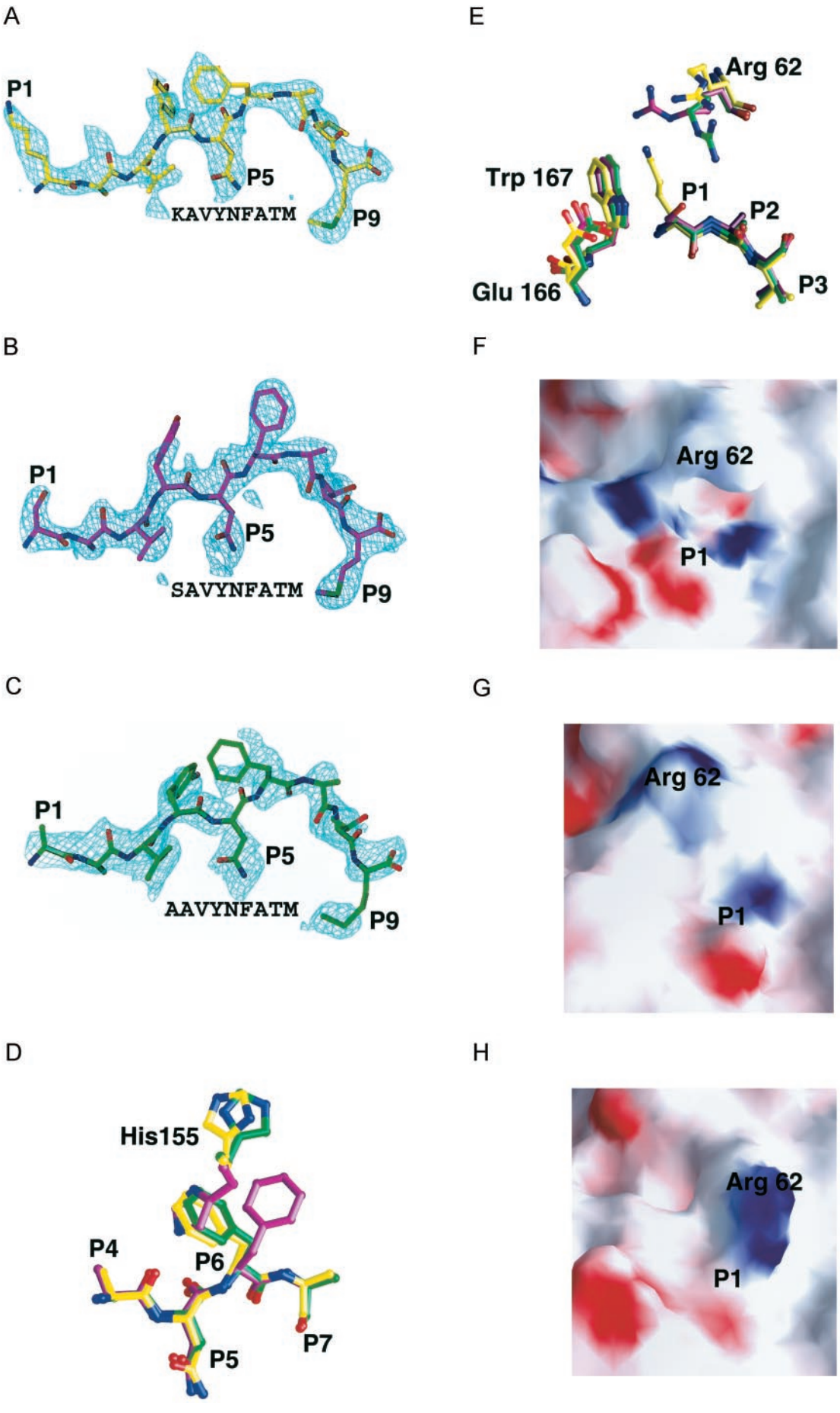

dependent on the sequence of the peptide. When T2D$^b$ cells were stained with mAb 28.8.6s, flow cytometry analysis showed that the D$^b$ molecules were detected by mAb 28.8.6s if peptides K1S, K1S/C9M, or K1A/C9M were bound. The same mAb failed to bind to D$^b$ molecules if the cells were incubated with gp33 or C9M (Fig. 6). These results suggest that a serine or alanine at position 1, in combination with residues in pocket A of the peptide-binding groove, form an epitope capable of recognition by mAb 28.8.6s, but the presence of lysine at P1 disrupts that epitope. Other P1 substitutions (D, E, F, L, N, R, W, or Y) also did not allow recognition (data not shown).

To visualize the differences in TCR and Ab recognition of gp33 and its variants and to examine the potential structural differences directly, we determined the crystallographic structures of three gp33/D$^b$ variants (C9M, K1A/C9M, and K1S/C9M). The K1A/C9M peptide was chosen because the substitution at P1 is similar in size to the K1S substitution, but the effect on B6 splenocyte recognition was significantly smaller than K1S (Fig. 1*B*). The molecular replacement solutions for all the three complexes were unambiguous. The models were refined in CNS and peptide was omitted during refinement and electron density calculations, until the $R_{work}$ was <30%, to reduce model bias. Manual intervention was performed with the model building software O. The final model for all the three structures has well-defined electron density with average real-space correlation coefficients of 75.7, 73.2, and 78.2% for C9M, K1A/C9M, and K1S/C9M, respectively. The final $R_{free}$ (50) is 28.6 from 50–2.7 Å for C9M, 29.2% from 50–2.65 Å for K1A/C9M, and 30.3% from 50–2.6 Å for K1S/C9M. The stereochemistry of all three structures is excellent, with no residues in disallowed regions of the Ramachandran plot.

In all three structures the main chain and side chain electron density for the peptide is well defined for all residues except for the side chain of the P4 Tyr, but even in that case the direction of the side chain is unambiguous (Fig. 7, *A–C*).

The structures of C9M, K1A/C9M, and K1S/C9M bound to D$^b$ are very similar. A major difference seen in the structures is the position of the Phe at P6 (Fig. 7). In the structure of C9M/D$^b$, the P6 Phe is directed back along the peptide main chain, interacting weakly with carbonyl oxygen at position 4. In the K1S/C9M structure the Phe rotates ~136 degrees about the bond defined by the c$\alpha$ and c$\beta$ carbons and is directed toward the solvent, as compared with its conformation in C9M. In a coordinated movement, His$^{155}$ of the $\alpha_2$ domain, which faces the solvent in C9M and K1A/C9M, has rotated ~133 degrees about the c$\alpha$-c$\beta$ bond to take the position previously occupied by the Phe at P6 in C9M and K1A/C9M (Fig. 7*D*). In K1S/C9M, His$^{155}$ makes a new hydrogen bond with the carbonyl oxygen of P4. In K1A/C9M, the Phe at position 6 has same conformation as that in C9M.

These rotations could explain altered recognition by the Abs and P14 TCR. Alternatively, the differences in the positions may be a crystallization artifact. We found no structural change at the P1 or P9 position that could account for the differences in the P6 Phe position. Additionally, there are no crystal contacts to the P6 Phe that could account for the different positions. We suggest that this change in the P6 position was due to a crystallization artifact. This hypothesis was based, in part, on the fact that the changes observed were all simple rotations of side chains for the Phe at P6 and His$^{155}$ and these types of rotations are seen frequently for these amino acids (51). The reactivity of K1S/C9M and K1A/C9M in B6 and P14 mice are very similar, suggesting that any structural difference should not be particularly large. It is possible that the energetic differences between the positions are very small to negligible, such that the position could be influenced by the activity of the solvent in the crystallization drops or that the position could be easily influenced by docking of the TCR. To test whether the structural changes at P6 were energetically similar, two peptides were constructed. Both Ala or Glu were substituted for Phe at the P6 position in the C9M peptide. If the position of the Phe is energetically favored in the observed position in C9M (pointed backwards toward the P4 carbonyl), we expect to see a decrease in peptide binding (or no change) by the substitution of the Phe side chain with a methyl group from alanine in F6A/C9M and a decrease in peptide binding in F6E/C9M due to charge repulsion from the interaction between the glutamate side chain and the P4 carbonyl. If the solvent-exposed position for P6 observed in K1S/C9M is energetically equivalent to the position observed in the C9M/D$^b$ structure, we expect to see no change in the peptide binding to D$^b$. Binding was measured and both F6E/C9M and F6A/C9M bind equivalently (data not shown). We interpret this to mean that the two P6 positions seen in the C9M and K1S/C9M crystal structures are not significantly energetically different. We also conclude either that the different positions seen in the crystal are a result of the activity of the solvent or that the substitutions at the P1 and P9 positions subtly affect the position of the P6 side chain. Although we cannot absolutely rule out the possibility that the P6 positions seen do not have an effect on T cell recognition, it does not seem likely. Thus, we conclude that the different positions of P6 Phe observed in the structures of K1S/C9M and C9M are not involved in the differences in the biological activity.

Comparing the interactions of C9M, K1A/C9M, and K1S/C9M with the peptide-binding cleft shows changes around position P1. The wild-type P1 lysine in C9M does not make any contacts with residues of binding cleft. The terminal nitrogen atom is completely solvent exposed but is surrounded by residues in the binding cleft out of Van der Waal contact distances. The serine at position 1 in K1S/C9M makes hydrogen bonds with Lys$^{66}$ and Glu$^{163}$ of D$^b$. A major change in K1S/C9M as compared with C9M is the conformation of Arg$^{62}$ of the $\alpha_1$ domain. The side chain of Arg$^{62}$ moves 3.8 Å toward the P1 position from the surface as compared with C9M (Fig. 7*E*). The distance between Arg$^{62}$ of K1S/C9M and lysine of peptide in the C9M structure is 2.5 Å. This suggests that the charge associated with the lysine side chain at P1 in C9M forces Arg$^{62}$ away from the P1 side chain toward the surface of the binding cleft. However, in K1S/C9M the P1 serine does not obstruct the movement of Arg$^{62}$. As a consequence of the smaller P1 side chains (alanine and serine), Trp$^{167}$ moves

**FIGURE 7.** The structures of the peptide variants show subtle structural changes at the termini that contribute to differences in T cell recognition. Omit electron density maps of C9M (KAVYNFATM) (*A*), K1S/C9M (SAVYNFATM) (*B*), and K1A/C9M (AAVYNFATM) (*C*) show that electron density is well defined for all three peptides. The omit maps are contoured at 1$\sigma$ with a cover radius of 1.5 Å. Superpositioning the peptide-binding clefts of the different structures shows residues that alter their positions by >1 Å. *D*, The P6 Phe in C9M (yellow) is rotated ~136 degrees from the position seen in K1S/C9M (magenta) or K1A/C9M (green) and the His$^{155}$ has rotated ~122 degrees to fill the position vacated by the Phe. *E*, Examination of the region about the P1 side chain shows that the side chain of Arg$^{62}$ in the structure of K1S/C9M (magenta) moves toward the binding cleft by 3.8 Å as compared with C9M (yellow). In the structure of K1A/C9M (green), the Arg$^{62}$ side chain flips in the other direction as compared with K1S/C9M by 2.7 Å and C9M. *F*, Surface representation around P1 site in C9M. *G*, Surface representation around P1 site of K1S/C9M. *H*, Surface representation around P1 site of K1A/C9M.

toward the P1 position in both K1S/C9M and K1A/C9M as compared with C9M (Fig. 7*E*). Therefore, there is a significant change in the molecular surface that the P14 TCR may contact in this area (Fig. 7, *F–H*). The major difference seen between K1S/C9M and K1A/C9M (similar activity to gp33) is the presence of a negatively charged bulge in K1S/C9M. All other changes appear to be inconsequential.

In summary, we have studied the impact of the N- and C-terminal peptide residues at the recognition of peptide by cytotoxic $CD8^+$ T cells. Although three of five class I MHC/TCR cocrystal structures do not show direct contacts with P1 and none shows direct contacts with the P9 position, our data indicate that the terminal residues of the epitope peptide contribute significantly to the interaction between TCR and the pMHC complex. T cell responses to target Ags can be modulated by conformational changes, which result in increased or decreased affinity of TCR to its ligands. Several approaches have been used to modulate immune responses. Franco et al. (52) have recently reported that high affinity of peptide Ag to class I MHC can increase the immune response of $CD8^+$ T cells and obviate the requirement for T cell help. Our data in this present study argue that the same goal could be achieved by increasing the affinity between TCR and the pMHC complex. This has been shown using the A6 TCR and alteration of an antagonist to an agonist by virtue of an improvement in the complementarity between the pMHC and the TCR (53). Improved affinity between class I MHC and specific TCR may be valuable in the development of improved CTL epitope immunotherapeutics. Indeed, it has been demonstrated by several studies that the affinity of TCR to the pMHC complex influences the activation and functional property of T cells (54–56). Our study may provide a molecular basis for the modulation of the T cell response to gp33 by P14.

## Acknowledgments

We thank the members of the Collins and Frelinger labs for stimulating conversations and Katherine Midkiff and Carie Barnes for excellent technical assistance.

## References

1. Yewdell, J. W., and J. R. Bennink. 1992. Cell biology of antigen processing and presentation to major histocompatibility complex class I molecule-restricted T lymphocytes. *Adv. Immunol. 52:1.*
2. Townsend, A., and H. Bodmer. 1989. Antigen recognition by class I-restricted T lymphocytes. *Annu. Rev. Immunol. 7:601.*
3. Fremont, D. H., M. Matsumura, E. A. Stura, P. A. Peterson, and I. A. Wilson. 1992. Crystal structures of two viral peptides in complex with murine MHC class I H-$2K^b$. *Science 257:919.*
4. Bjorkman, P. J., M. A. Saper, B. Samraoui, W. S. Bennett, J. L. Strominger, and D. C. Wiley. 1987. The foreign antigen binding site and T cell recognition regions of class I histocompatibility antigens. *Nature 329:512.*
5. Bjorkman, P. J., M. A. Saper, B. Samraoui, W. S. Bennett, J. L. Strominger, and D. C. Wiley. 1987. Structure of the human class I histocompatibility antigen, HLA-A2. *Nature 329:506.*
6. Collins, E. J., D. N. Garboczi, and D. C. Wiley. 1994. Three-dimensional structure of a peptide extending from one end of a class I MHC binding site. *Nature 371:626.*
7. Madden, D. R., J. C. Gorga, J. L. Strominger, and D. C. Wiley. 1992. The three-dimensional structure of HLA-B27 at 2.1 Å resolution suggests a general mechanism for tight peptide binding to MHC. *Cell 70:1035.*
8. Garrett, T. P., M. A. Saper, P. J. Bjorkman, J. L. Strominger, and D. C. Wiley. 1989. Specificity pockets for the side chains of peptide antigens in HLA-Aw68. *Nature 342:692.*
9. Batalia, M. A., and E. J. Collins. 1997. Peptide binding by class I and class II MHC molecules. *Biopoly 43:281.*
10. Saper, M. A., P. J. Bjorkman, and D. C. Wiley. 1991. Refined structure of the human histocompatibility antigen HLA-A2 at 2.6 Å resolution. *J. Mol. Biol. 219:277.*
11. Guo, H. C., D. R. Madden, M. L. Silver, T. S. Jardetzky, J. C. Gorga, J. L. Strominger, and D. C. Wiley. 1993. Comparison of the P2 specificity pocket in three human histocompatibility antigens: HLA-A*6801, HLA-A*0201, and HLA-B*2705. *Proc. Natl. Acad. Sci. USA 90:8053.*
12. Jardetzky, T. S., W. S. Lane, R. A. Robinson, D. R. Madden, and D. C. Wiley. 1991. Identification of self peptides bound to purified HLA-B27. *Nature 353:326.*
13. Falk, K., O. Rötzschke, S. Stevanovic, G. Jung, and H.-G. Rammensee. 1991. Allele-specific motifs revealed by sequencing of self-peptides eluted from MHC molecules. *Nature 351:290.*
14. Garboczi, D. N., and W. E. Biddison. 1999. Shapes of MHC restriction. *Immunity 10:1.*
15. Garcia, K. C., L. Teyton, and I. A. Wilson. 1999. Structural basis of T cell recognition. *Annu. Rev. Immunol. 17:369.*
16. Wilson, I. A., and K. C. Garcia. 1997. T-cell receptor structure and TCR complexes. *Curr. Opin. Struct. Biol. 7:839.*
17. Reiser, J. B., C. Darnault, A. Guimezanes, C. Gregoire, T. Mosser, A. M. Schmitt-Verhulst, J. C. Fontecilla-Camps, B. Malissen, D. Housset, and G. Mazza. 2000. Crystal structure of a T cell receptor bound to an allogeneic MHC molecule. *Nat. Immunol. 1:291.*
18. Ding, Y. H., B. M. Baker, D. N. Garboczi, W. E. Biddison, and D. C. Wiley. 1999. Four A6-TCR/peptide/HLA-A2 structures that generate very different T cell signals are nearly identical. *Immunity 11:45.*
19. Ding, Y. H., K. J. Smith, D. N. Garboczi, U. Utz, W. E. Biddison, and D. C. Wiley. 1998. Two human T cell receptors bind in a similar diagonal mode to the HLA- A2/Tax peptide complex using different TCR amino acids. *Immunity 8:403.*
20. Garboczi, D. N., P. Ghosh, U. Utz, Q. R. Fan, W. E. Biddison, and D. C. Wiley. 1996. Structure of the complex between human T-cell receptor, viral peptide and HLA-A2. *Nature 384:134.*
21. Garcia, K. C., M. Degano, L. R. Pease, M. Huang, P. A. Peterson, L. Teyton, and I. A. Wilson. 1998. Structural basis of plasticity in T cell receptor recognition of a self peptide-MHC antigen. *Science 279:1166.*
22. Garcia, K. C., M. Degano, R. L. Stanfield, A. Brunmark, M. R. Jackson, P. A. Peterson, L. Teyton, and I. A. Wilson. 1996. An $\alpha\beta$ T cell receptor structure at 2.5 Å and its orientation in the TCR-MHC complex. *Science 274:209.*
23. Jorgensen, J. L., U. Esser, B. Fazekas de St Groth, P. A. Reay, and M. M. Davis. 1992. Mapping T-cell receptor-peptide contacts by variant peptide immunization of single-chain transgenics. *Nature 355:224.*
24. Pircher, H., K. Burki, R. Lang, H. Hengartner, and R. M. Zinkernagel. 1989. Tolerance induction in double specific T-cell receptor transgenic mice varies with antigen. *Nature 342:559.*
25. Zhao, R., D. Loftus, E. Appella, and E. J. Collins. 1999. Structural evidence of T cell xenoreactivity in the absence of molecular mimicry. *J. Exp. Med. 189:359.*
26. Wang, B., R. Maile, R. Greenwood, E. J. Collins, and J. A. Frelinger. 2000. Naive $CD8^+$ T cells do not require costimulation for proliferation and differentiation into cytotoxic effector cells. *J. Immunol. 164:1216.*
27. Pogue, R., J. Eron, J. Frelinger, and M. Matsui. 1995. Amino-terminal alteration of the HLA-A*0201-restricted human immunodeficiency virus pol peptide increases complex stability and in vitro immunogenicity. *Proc. Natl. Acad. Sci. USA 92:8166.*
28. Salter, R., D. Howell and P. Cresswell. 1985. Genes regulating HLA class I antigen expression in T-B lymphoblast hybrids. *Immunogenetics 21:235.*
29. Ozato, K., N. Mayer, and D. H. Sachs. 1980. Hybridoma cell lines secreting monoclonal antibodies to mouse H-2 and $I^a$ antigens. *J. Immunol. 124:533.*
30. Ozato, K., and D. H. Sachs. 1981. Monoclonal antibodies to mouse MHC antigens. III. Hybridoma antibodies reacting to antigens of the H-$2^b$ haplotype reveal genetic control of isotype expression. *J. Immunol. 126:317.*
31. Otwinowski, Z., and W. Minor. 1996. Processing of X-ray diffraction data collected in oscillation mode. In *Methods in Enzymology*, Vol. 276. C. W. J. Carter and R. M. Sweet, eds. Academic, New York, p. 307.
32. Dodson, E. J., M. Winn, and A. Ralph. 1998. Collaborative computational project number 4: providing programs for protein crystallography. *Methods Enzymol. 277:620.*
33. Jones, T. A., J.-Y. Zou, S. W. Cowan, and M. Kjeldgaard. 1991. Improved methods for building protein models in electron density maps and the location of errors in these models. *Acta Crystallogr. A47:110.*
34. Murali-Krishna, K., J. D. Altman, M. Suresh, D. J. Sourdive, A. J. Zajac, J. D. Miller, J. Slansky, and R. Ahmed. 1998. Counting antigen-specific CD8 T cells: a reevaluation of bystander activation during viral infection. *Immunity 8:177.*
35. Blattman, J. N., D. J. Sourdive, K. Murali-Krishna, R. Ahmed, and J. D. Altman. 2000. Evolution of the T cell repertoire during primary, memory, and recall responses to viral infection. *J. Immunol. 165:6081.*
36. Gairin, J. E., H. Mazarguil, D. Hudrisier, and M. B. Oldstone. 1995. Optimal lymphocytic choriomeningitis virus sequences restricted by H-$2D^b$ major histocompatibility complex class I molecules and presented to cytotoxic T lymphocytes. *J. Virol. 69:2297.*
37. Ruppert, J., J. Sidney, E. Celis, R. T. Kubo, H. M. Grey, and A. Sette. 1993. Prominent role of secondary anchor residues in peptide binding to HLA-A2.1 molecules. *Cell 74:929.*
38. Colbert, R. A., S. L. Rowland-Jones, A. J. McMichael, and J. A. Frelinger. 1994. Differences in peptide presentation between B27 subtypes: the importance of the P1 side chain in maintaining high affinity peptide binding to B*2703. *Immunity 1:121.*
39. Bowness, P., R. L. Allen, and A. J. McMichael. 1994. Identification of T cell receptor recognition residues for a viral peptide presented by HLA B27. *Eur. J. Immunol. 24:2357.*
40. Lim, D. G., K. Bieganowska Bourcier, G. J. Freeman, and D. A. Hafler. 2000. Examination of $CD8^+$ T cell function in humans using MHC class I tetramers: similar cytotoxicity but variable proliferation and cytokine production among different clonal $CD8^+$ T cells specific to a single viral epitope. *J. Immunol. 165:6214.*

41. Bosselut, R., S. Kubo, T. Guinter, J. L. Kopacz, J. D. Altman, L. Feigenbaum, and A. Singer. 2000. Role of CD8$\beta$ domains in CD8 coreceptor function: importance for MHC I binding, signaling, and positive selection of $CD8^+$ T cells in the thymus. *Immunity 12:409.*
42. Garcia, K. C., C. A. Scott, A. Brunmark, F. R. Carbone, P. A. Peterson, I. A. Wilson, and L. Teyton. 1996. CD8 enhances formation of stable T-cell receptor/MHC class I molecule complexes. *Nature 384:577.*
43. Norment, A. M., and D. R. Littman. 1988. A second subunit of CD8 is expressed in human T cells. *EMBO J. 7:3433.*
44. Daniels, M. A., and S. C. Jameson. 2000. Critical role for CD8 in T cell receptor binding and activation by peptide/major histocompatibility complex multimers. *J. Exp. Med. 191:335.*
45. Vidal, K., C. Daniel, M. Hill, D. R. Littman, and P. M. Allen. 1999. Differential requirements for CD4 in TCR-ligand interactions. *J. Immunol. 163:4811.*
46. Bluestone, J. A., S. Jameson, S. Miller, and R. Dick. 1992. Peptide-induced conformational changes in class I heavy chains alter major histocompatibility complex recognition. *J. Exp. Med. 176:1757.*
47. Hogquist, K. A., S. C. Jameson, and M. J. Bevan. 1995. Strong agonist ligands for the T cell receptor do not mediate positive selection of functional $CD8^+$ T cells. *Immunity 3:79.*
48. Sakaguchi, T., Y. Takamiya, M. Edidin, K. Nokihara, K. Miwa, C. Schonbach, and M. Takiguchi. 1998. Crucial role of N-terminal residue of binding peptides in recognition of the monoclonal antibody specific for the peptide-HLA-B5, -B35 complex. *Immunogenetics 47:149.*
49. Allen, H., J. Fraser, D. Flyer, S. Calvin, and R. Flavell. 1986. $\beta_2$-microglobulin is not required for cell surface expression of the murine class I histocompatibility antigen $H\text{-}2D^b$ or of a truncated $H\text{-}2D^b$. *Proc. Natl. Acad. Sci. USA 83:7447.*
50. Adams, P. D., N. S. Pannu, R. J. Read, and A. T. Brunger. 1997. Cross-validated maximum likelihood enhances simulated annealing refinement. *Proc. Natl. Acad. Sci. USA 94:5018.*
51. Lovell, S. C., J. M. Word, J. S. Richardson, and D. C. Richardson. 2000. The penultimate rotamer library. *Proteins 40:389.*
52. Franco, A., D. A. Tilly, I. Gramaglia, M. Croft, L. Cipolla, M. Meldal, and H. M. Grey. 2000. Epitope affinity for MHC class I determines helper requirement for CTL priming. *Nat. Immunol. 1:145.*
53. Baker, B. M., S. J. Gagnon, W. E. Biddison, and D. C. Wiley. 2000. Conversion of a T cell antagonist into an agonist by repairing a defect in the TCR/peptide/MHC interface: implications for TCR signaling. *Immunity 13:475.*
54. Constant, S., C. Pfeiffer, A. Woodard, T. Pasqualini, and K. Bottomly. 1995. Extent of T cell receptor ligation can determine the functional differentiation of naive $CD4^+$ T cells. *J. Exp. Med. 182:1591.*
55. Malherbe, L., C. Filippi, V. Julia, G. Foucras, M. Moro, H. Appel, K. Wucherpfennig, J. C. Guery, and N. Glaichenhaus. 2000. Selective activation and expansion of high-affinity $CD4^+$ T cells in resistant mice upon infection with *Leishmania major*. *Immunity 13:771.*
56. Slansky, E. J., M. F. Rattis, F. L. Boyd, T. Fahmy, M. E. Jaffee, P. J. Schneck, H. D. Margulies, and M. D. Pardoll. 2000. Enhanced antigen-specific antitumor immunity with altered peptide ligands that stabilize the MHC-peptide-TCR complex. *Immunity 13:529.*